Research Article

Rapid Communications in Mass Spectrometry

Received: 14 December 2014 Revised: 16 February 2015 Accepted: 18 February 2015 Published online in Wiley Online Library

Rapid Commun. Mass Spectrom. **2015**, *29*, 901–909
(wileyonlinelibrary.com) DOI: 10.1002/rcm.7175

Non-linear mixing effects on mass-47 CO_2 clumped isotope thermometry: Patterns and implications

William F. Defliese[1,2]* and Kyger C. Lohmann[1]

[1]Department of Earth and Environmental Sciences, University of Michigan, 1100 North University Ave, Ann Arbor, MI 48103, USA
[2]Department of Earth, Planetary, and Space Sciences, University of California, Los Angeles, 595 Charles Young Drive East, Los Angeles, CA 90095, USA

RATIONALE: Mass-47 CO_2 clumped isotope thermometry requires relatively large (~20 mg) samples of carbonate minerals due to detection limits and shot noise in gas source isotope ratio mass spectrometry (IRMS). However, it is unreasonable to assume that natural geologic materials are homogenous on the scale required for sampling. We show that sample heterogeneities can cause offsets from equilibrium Δ_{47} values that are controlled solely by end member mixing and are independent of equilibrium temperatures.
METHODS: A numerical model was built to simulate and quantify the effects of end member mixing on Δ_{47}. The model was run in multiple possible configurations to produce a dataset of mixing effects. We verified that the model accurately simulated real phenomena by comparing two artificial laboratory mixtures measured using IRMS to model output.
RESULTS: Mixing effects were found to be dependent on end member isotopic composition in $\delta^{13}C$ and $\delta^{18}O$ values, and independent of end member Δ_{47} values. Both positive and negative offsets from equilibrium Δ_{47} can occur, and the sign is dependent on the interaction between end member isotopic compositions. The overall magnitude of mixing offsets is controlled by the amount of variability within a sample; the larger the disparity between end member compositions, the larger the mixing offset.
CONCLUSIONS: Samples varying by less than 2 ‰ in both $\delta^{13}C$ and $\delta^{18}O$ values have mixing offsets below current IRMS detection limits. We recommend the use of isotopic subsampling for $\delta^{13}C$ and $\delta^{18}O$ values to determine sample heterogeneity, and to evaluate any potential mixing effects in samples suspected of being heterogonous. Copyright © 2015 John Wiley & Sons, Ltd.

Use of the mass-47 CO_2 clumped isotope thermometer has expanded greatly in the last few years, being applied to a diverse set of proxy materials. These materials include mollusks,[1–3] brachiopods,[4] corals,[5,6] speleothems,[7,8] foraminifera,[9] soil carbonates,[10–12] phosphate-associated carbonate,[13] and various diagenetic phases including phreatic and burial cements[14,15] and dolomite.[16,17] To achieve high-quality measurements, counting statistics requires large sample sizes, with typical replicates of 5–15 mg being analyzed multiple times for total sample sizes of up to 50 mg.[18] Alternatively, some researchers have applied techniques that use multiple (10+) aliquots of 150–200 μg of carbonate material, thus reducing the sample size to approximately 2 mg per replicate, although with a slight loss in sensitivity and throughput.[19,20]

Most of the phases used in clumped isotope studies show isotopic heterogeneity on a small scale, such as the seasonal growth bands in many biogenic carbonates, and multiple stages of cementation in diagenetic carbonates, soil carbonates, and speleothems. Sampling procedures use either a drill or mortar and pestle to extract large quantities of sample powder, and can combine multiple growth bands or cement layers to reach the required amount. This leads to homogenization of an isotopically heterogeneous sample, each layer with potentially distinct values for $\delta^{13}C$, $\delta^{18}O$, and Δ_{47}. Given that Δ_{47} is calculated relative to the sample's bulk $\delta^{13}C$ and $\delta^{18}O$ values, mixing phases with different compositions can have a dramatic effect on the calculated Δ_{47} values, and thus on calculated paleotemperatures.

Mixing relationships in multiply substituted isotopologues have been investigated by a number of authors, particularly focusing on the isotopologues of CO_2[21–23] and N_2O,[24] with only a few studies briefly considering $CaCO_3$.[2,16] These studies have shown that mixing of two different populations of CO_2 (or N_2O) causes deviations in measured isotope ratios from what would be expected from a linear mixing model. For example, Affek and Eiler[23] demonstrated that mixing of CO_2 from car exhaust and ambient atmosphere produced Δ_{47} offsets of up to 0.042‰ compared with a linear mixing model, while Henkes *et al.*[2] suggested a maximum offset of 0.0014‰ in a hypothetical bivalve. In each of these examples, mixing effects would create an underestimate of the average equilibrium temperature, and they can be larger than typical analytical errors for Δ_{47} measurement, such as the 0.017‰ standard deviation reported for interlaboratory comparison of NBS-19 by Dennis *et al.*[25] While it has been well documented that certain proxy materials, such as speleothems and corals,

* *Correspondence to:* W. F. Defliese, Department of Earth and Environmental Sciences, University of Michigan, 1100 North University Ave, Ann Arbor, MI 48103, USA.
E-mail: wdefliese@gmail.com

show Δ_{47}-based temperatures that deviate from known average growth temperatures, the reasons for this are unclear. Several possibilities have been invoked to account for these discrepancies, such as disequilibrium precipitation, diagenetic overprinting, or biologic effects on precipitation, but it is possible that non-linear mixing can account for some of these observed deviations.

This paper builds on the prior work with isotopologues of CO_2, and attempts to quantify the magnitude of temperature estimate bias that occurs when carbonates of different bulk isotopic composition are mixed. Specifically, we establish the scale on which mixing becomes significant compared with measurement error, and investigate whether this biasing can account for some of the discrepancies reported thus far in the literature. We establish the scale and implications of mixing on Δ_{47} values by simulating the effects of mixing, utilizing a numerical model, and test it with laboratory measurements of mixtures of carbonates with divergent end member compositions. We also provide a process and worksheet for other workers to calculate potential mixing offsets in their own investigations using clumped isotope techniques.

EXPERIMENTAL

Theory of mixing

Prior work[16,22,23] has demonstrated that a mixture of CO_2 of different compositions mixes linearly with respect to $\delta^{13}C$, $\delta^{18}O$, δ^{45}, δ^{46}, and δ^{47} values, but that Δ_{47} mixes non-linearly. Our model calculates the Δ_{47} value of a mixture by calculating the Δ_{47}, $\delta^{13}C$, $\delta^{18}O$, δ^{45}, δ^{46}, and δ^{47} values of each end member relative to a working gas and instrument, assuming linear mixing of the $\delta^{13}C$, $\delta^{18}O$, δ^{45}, δ^{46}, and δ^{47} values, and calculates the Δ_{47} value of the mixture using these derived values. For each end member, we begin by assigning a value for Δ_{47}, $\delta^{13}C$, and $\delta^{18}O$, which is used to calculate the δ^{45}, δ^{46}, and δ^{47} values of the CO_2 gas produced by phosphoric acid digestion relative to a working gas. The $\delta^{18}O$ values for CO_2 gas are calculated by using the phosphoric acid digestion calibration of Swart *et al.*[26] The $\delta^{13}C$ value is assumed to not fractionate during acid digestion. The gas values of $\delta^{13}C$ and $\delta^{18}O$ were used to calculate R^{13} and R^{18} for each end member, using the absolute abundance ratios of Gonfiantini *et al.*:[27]

$$R^{13} = \left(\frac{\delta^{13}C_{VPDB}}{1000} + 1\right) \times 0.0112372 \quad (1)$$

$$R^{18} = \left(\frac{\delta^{18}O_{VSMOW}}{1000} + 1\right) \times 0.0020052 \quad (2)$$

R^{17} was calculated based on R^{18}, using:

$$R^{17} = \left(\frac{R^{18}}{0.0020052}\right)^{0.5164} \times 0.0003799 \quad (3)$$

The absolute abundance of each isotope was then calculated for each end member:

$$[^{12}C] = \frac{1}{1 + R^{13}} \quad (4)$$

$$[^{13}C] = \frac{R^{13}}{1 + R^{13}} \quad (5)$$

$$[^{16}O] = \frac{1}{1 + R^{17} + R^{18}} \quad (6)$$

$$[^{17}O] = \frac{R^{17}}{1 + R^{17} + R^{18}} \quad (7)$$

$$[^{18}O] = \frac{R^{18}}{1 + R^{17} + R^{18}} \quad (8)$$

These abundances are used to calculate the stochastic distribution of isotopes, R^*, which is the ratio of the mass abundance of each isotopologue relative to the mass 44 abundance:

$$R^{45*} = \frac{[^{13}C][^{16}O][^{16}O] + 2[^{12}C][^{16}O][^{17}O]}{[^{12}C][^{16}O][^{16}O]} \quad (9)$$

$$R^{46*} = \frac{2[^{12}C][^{16}O][^{18}O] + [^{12}C][^{17}O][^{17}O] + 2[^{13}C][^{16}O][^{17}O]}{[^{12}C][^{16}O][^{16}O]} \quad (10)$$

$$R^{47*} = \frac{2[^{13}C][^{16}O][^{18}O] + [^{13}C][^{17}O][^{17}O] + 2[^{12}C][^{17}O][^{18}O]}{[^{12}C][^{16}O][^{16}O]} \quad (11)$$

The same steps are taken for the working gas to calculate the stochastic distribution of isotopes, R^*_{WG}. The δ^{45} and δ^{46} values are then calculated for both end members as follows:

$$\delta^{45} = \left(\frac{R^{45*}}{R^{45*}_{WG}} - 1\right) \times 1000 \quad (12)$$

$$\delta^{46} = \left(\frac{R^{46*}}{R^{46*}_{WG}} - 1\right) \times 1000 \quad (13)$$

Finally, the δ^{47} value was calculated for each end member by taking the Δ_{47} value for each, removing the acid fractionation offset and empirical transfer function (ETF), and making the assumption that only the δ^{47} value contributes to the Δ_{47} measurements, as the abundances of ^{17}O are very low compared with those of ^{18}O.[28] This assumption introduces a small error in the calculations; however, when mixtures of known compositions were analyzed on the mass spectrometer, the difference between the measured and calculated δ^{47} values was ≤0.02‰. For each end member, using the nomenclature of Dennis *et al.*,[25] and with the end member values chosen for Δ_{47}, the steps were:

$$\Delta_{47[RF]} = \Delta_{47[\text{End Member Value}]} - \text{acid correction} \quad (14)$$

$$\Delta_{47[SGvsWG]0} = \frac{\Delta_{47[RF]} - ETF_{Int}}{ETF_{Slope}} \quad (15)$$

where ETF_{Int} and ETF_{Slope} represent the intercept and slope of the empirical transfer function, $\Delta_{47[RF]}$ is the Δ_{47} value in the universal reference frame, and $\Delta_{47[SGvsWG]0}$ is the equilibrated gas corrected Δ_{47} value. The δ^{47} value was calculated using the following equation, whose derivation is outlined in Appendix A:

Rapid Communications in Mass Spectrometry

$$\delta^{47} = \frac{(\Delta_{47[SGvsWG]0} + 1000) \times R^{47*} - 1000 \times R^{47*}_{WG}}{R^{47*}_{WG} - EGL_{Slope} \times R^{47*}} \quad (16)$$

where EGL_{Slope} is the slope of the equilibrated gas lines.

For each mixture, linear mixing was assumed for the $\delta^{13}C$, $\delta^{18}O$, δ^{45}, δ^{46}, and δ^{47} values. The values for each mixture were calculated by:

$$\delta i_{mix} = x_1 \delta i_1 + x_2 \delta i_2 \ldots + x_n \delta i_n \quad (17)$$

where δi represents a given component, n represents the end member compositions, and x is the fractional contribution of each end member, with $\Sigma_x = 1$. From here, the normal process of calculating $R^{45*}{}_{mix}$, $R^{46*}{}_{mix}$, and $R^{47*}{}_{mix}$ is performed with the stochastic distribution of isotopes in the mixture based on $\delta^{13}C_{mix}$ and $\delta^{18}O_{mix}$ values using Eqns. (1–11). The $\delta^{45}{}_{mix}$, $\delta^{46}{}_{mix}$, and $\delta^{47}{}_{mix}$ values are used to calculate $R^{45}{}_{mix}$, $R^{46}{}_{mix}$, and $R^{47}{}_{mix}$ by the following equation:

$$R^i = \left(\frac{\delta i}{1000} + 1\right) \times R^{i*}_{WG} \quad (18)$$

where i represents masses 45, 46 and 47. Finally, Δ_{47mix} is calculated as:

$$\Delta_{47[SGvsWG]mix} = \left[\left(\frac{R^{47}}{R^{47*}} - 1\right) - \left(\frac{R^{46}}{R^{46*}} - 1\right) - \left(\frac{R^{45}}{R^{45*}} - 1\right)\right] \times 1000 \quad (19)$$

$$\Delta_{47[SGvsWG]0mix} = \Delta_{47[SGvsWG]mix} - \delta^{47}{}_{mix} \times EGL_{Slope} \quad (20)$$

$$\Delta_{47mix} = \Delta_{47[SGvsWG]0mix} \times ETF_{Slope} + ETF_{Int} \quad (21)$$

The choice of working gas, acid reaction temperature, and machine artifacts (taken into account with the Empirical Reference Frame) affects the calculated values for δ^{45}, δ^{46}, and δ^{47}, but does not affect the final calculated $\delta^{13}C$, $\delta^{18}O$, and Δ_{47} values.

Model and data generation

Using the technique and equations described above, a numerical model (see Supporting Information for model worksheet) was constructed to calculate the effect of mixing end member carbonates with differing compositions. To investigate general patterns and trends caused by mixing solid carbonates, simulations were performed representing a wide spectrum of end member compositions and equilibrium temperatures. For these simulations, we assumed an 'ideal' machine and working gas, with working gas composition of $\delta^{13}C$ = 0‰ VPDB and $\delta^{18}O$ = 0‰ VSMOW, ETF_{Slope} = 1, ETF_{Int} = 0, EGL_{Slope} = 0, and acid reaction at 25 °C. (In practice, users should use the appropriate values for their system and operating conditions.) Under these conditions, the chosen end member value for Δ_{47} is equivalent to $\Delta_{47[SGvsWG]}$ and Eqns. (14) and (15) are unnecessary. In addition, Eqn. (16) simplifies to take the form:

$$\delta^{47} = \left(\left(\frac{\Delta_{47[SGvsWG]0}}{1000} + 1\right) \times \left(\frac{R^{47*}}{R^{47*}_{WG}}\right) - 1\right) \times 1000 \quad (22)$$

We analyzed numerous scenarios involving mixing of end members of differing bulk isotopic compositions, mixing proportions, and equilibrium temperatures. For simplicity, we chose to use three values of Δ_{47} for end members: 0.55198, 0.71324, and 0.77718 (corresponding to 100, 20 and 0 °C on the Dennis and Schrag[29] temperature calibration, as corrected in Dennis *et al.*[25]) We used values for $\delta^{13}C$ and $\delta^{18}O$ that ranged from +15‰ to −15‰ VPDB, and investigated the effects of each. Eight different scenarios for mixing were considered: (1) constant Δ_{47}, with variation in $\delta^{13}C$ and $\delta^{18}O$ bulk composition with both offset in the same positive or negative direction; (2) constant Δ_{47} and $\delta^{13}C$ values, but with variation in $\delta^{18}O$ values; (3) constant Δ_{47} and $\delta^{18}O$ values, with variation in $\delta^{13}C$ values; (4) constant Δ_{47}, but where the $\delta^{13}C$ and $\delta^{18}O$ values varied in opposite directions; (5) different Δ_{47} with constant $\delta^{13}C$ and $\delta^{18}O$ values; (6) different Δ_{47} with variation in $\delta^{13}C$ and $\delta^{18}O$ values moving in the same direction; (7) different Δ_{47} with either $\delta^{13}C$ or $\delta^{18}O$ values constant; and (8) different Δ_{47} with variation in $\delta^{13}C$ and $\delta^{18}O$ values moving in opposite directions. Simulations were run for mixing proportions of x = 0 to 1 in 0.1 intervals.

Empirical test of mixing

To validate the simulations of our mixing model, an empirical test of mixing was performed. Mixture A consisted of a 1:1 mixture of laboratory standards Merck (Thermo Scientific, Inc.) and Carrara Marble (Quarry tailings, Carrara, Italy), while mixture B consisted of a 1:1 mixture of two field-collected samples, 10SP06A (Member B, Sheep Pass Formation, Nevada, USA, Late Cretaceous – Eocene) and *Otala lactea* (Bierman's Quarry, Bermuda, the shell carbonate of a recent land snail). Both mixtures were designed to create large mixing offsets to allow easy comparison with model results. The mixtures were prepared by weighing 50 mg powder of each end member, placing both powders into a sample vial, and shaking vigorously for several minutes. Both mixtures and all end members were analyzed for their $\delta^{13}C$, $\delta^{18}O$, and Δ_{47} values at the University of Michigan Stable Isotope Lab. The samples were digested with 105 wt % phosphoric acid at 75 °C in a common acid bath attached to a custom-built extraction line.[30] Sample CO_2 was purified by two stages of cryogenic separation at −90 °C to remove water, and the remaining contaminants were removed by passing the CO_2 through a column of PoraPak Q resin (Waters Corp., Milford, MA, USA; 50–80 mesh) held at −30 °C. Purified sample CO_2 was analyzed using a ThermoFinnigan MAT 253 isotope ratio mass spectrometer operated in dual-inlet mode as described in Huntington *et al.*[18] The samples were corrected for non-linearity and scale compression by use of an empirical transfer function as described in Dennis *et al.*,[25] which was constructed from standard CO_2 gases equilibrated at 25 and 1000 °C.

The measured end member values for both mixtures A and B were used as inputs for the mixing model, as well as the operating conditions for the instrument during the time that the samples were analyzed (October 23 to November 5, 2013). We used a working gas with values $\delta^{13}C$ = −3.70 VPDB, $\delta^{18}O$ = 34.99 VSMOW, the equilibrated gas slope was 0.0274 with a 1000 °C intercept of −0.8885, and the empirical transfer function slope was 1.0391 with an intercept of 0.9499. We used an empirically measured phosphoric acid fractionation offset of 0.067‰ for Δ_{47} and an α of 1.008051 for the $\delta^{18}O$ value to correct for digestion at 75 °C.[30]

RESULTS

The results from the mixing model simulations are presented in the Supporting Information. Empirical results from the laboratory mixtures and associated mixing model simulations are presented in Table 1, with all measured Δ_{47} values falling within error of model outputs.

DISCUSSION

General patterns and trends of mixing

We introduce a new term to describe the discrepancy between the Δ_{47} calculated by the model and the Δ_{47} calculated from conservative linear mixing of end member values. Since Δ is already in use, we use the greek letter Γ to describe this term, with $\Gamma_{47} = \Delta_{47Model} - \Delta_{47Linear}$ (Fig. 1). This will produce a positive value when conservative linear mixing underestimates Δ_{47}, and a negative value when linear mixing overestimates Δ_{47}. The units of Γ_{47} are ‰, and are equal to those of Δ_{47}.

Several general trends are immediately clear upon reviewing the data. First, the sign of Γ_{47} is controlled by the end member values of $\delta^{13}C$ and $\delta^{18}O$, and is independent of each end member's Δ_{47} value (Fig. 2). When the $\delta^{13}C$ and $\delta^{18}O$ values have a positive correlation, i.e. both values for one end member are more negative than the other, Γ_{47} is positive (Fig. 2(A)). Likewise, when one of either the $\delta^{13}C$ or $\delta^{18}O$ value is constant, and the other changes, Γ_{47} is positive (Fig. 2(B)). Γ_{47} is negative when the $\delta^{13}C$ and $\delta^{18}O$ values show a negative correlation, i.e. when one end member has positive $\delta^{13}C$ and negative $\delta^{18}O$ values, and the other end member has a negative $\delta^{13}C$ and a positive $\delta^{18}O$ value (Fig. 2(C)). Γ_{47} is zero and follows a linear mixing model when the end members have identical bulk isotopic compositions, regardless of Δ_{47} values (Fig. 2(D)). The implications are that apparent Δ_{47} values from mixtures can be an overestimate or underestimate of true temperature conditions, and deciphering which is true requires detailed knowledge of the correlation between the $\delta^{13}C$ and $\delta^{18}O$ values within the sample.

The magnitude of Γ_{47} is controlled by the size of the offset in the $\delta^{13}C$ and $\delta^{18}O$ values between the end members in the mixture, as well as the percentage contribution of each. In two-component mixing, the maximum size of Γ_{47} is reached when each end member contributes 50% to the final mixture, regardless of the sign of Γ_{47}. A plot of Γ_{47} versus x has a parabolic shape, which means that even small contributions from one end member have a significant contribution. For instance, a 1% contribution from one end member with 99% of the other gives a Γ_{47} value that is approximately 3.96% of the maximum, whereas a 5% contribution gives a Γ_{47} value that is 19% of the maximum. The maximum value of Γ_{47} depends primarily on the size of the offset between the $\delta^{13}C$ and $\delta^{18}O$ values of each end member, with a much smaller dependence on the actual $\delta^{13}C$ and $\delta^{18}O$ values for each end member. Larger offsets between the end members lead to a larger Γ_{47} value (Fig. 3), with an offset of 15‰ for the $\delta^{13}C$ and $\delta^{18}O$ values yielding a Γ_{47} value that is almost 9 times that obtained with an offset of 5‰ for both. An offset of 2‰ for both carbon and oxygen ratios leads to a Γ_{47} value of about 0.0010‰, which is comparable with the error for most measurements.

The actual carbon and oxygen isotope ratio values of each end member also make a much smaller but detectable difference in Γ_{47}. For example, a 15‰ offset between end members with both end members having positive $\delta^{13}C$ and $\delta^{18}O$ values makes for a smaller Γ_{47} than a 15‰ offset with both end members having negative $\delta^{13}C$ and $\delta^{18}O$ values (Fig. 4), and a Γ_{47} difference of 0.0017‰ is obtained for the case in Fig. 4. This is because there are many more stochastic ^{13}C–^{18}O bonds when both isotopes are abundant, which lessens the overexpression of ^{13}C–^{18}O bonds. The Δ_{47} value of each end member has an extremely small effect on the magnitude of Γ_{47}, and over the Δ_{47} values that we chose the maximum Γ_{47} was about 0.0001‰, when comparing end members with Δ_{47} = 0.77718 and 0.55198‰. This value is very small, and is within the shot noise limit for Δ_{47} measurement, so it can be effectively ignored.

Empirical test of the mixing model

The measured Δ_{47} results for both mixtures fall within one standard error of the predicted mean model result, and the errors are contained within the range of model runs (Fig. 5). The $\delta^{18}O$ and $\delta^{13}C$ results for mixture A fall slightly off the prediction for a 50:50 mixture of end members, indicating a slight sampling bias or that the mixture was not completely homogenized. This does not significantly affect the results,

Table 1. Clumped isotope results and model results

	n[a]	Δ_{47}	$\delta^{18}O$ (‰)	$\delta^{13}C$ (‰)
Carrara Marble	6	0.388±0.009	−2.26±0.12	1.73±0.10
Merck	4	0.609±0.017	−15.93±0.07	−34.86±0.17
Mixture A	6	0.641±0.009	−9.64±0.15	−17.89±0.24
Model (Mixture A)[b]	N/A	0.643	−9.09	−16.56
Otala lactea	4	0.700±0.013	−0.32±0.12	−9.79±0.01
10SP06A	4	0.686±0.012	−11.11±0.17	3.60±0.12
Mixture B	6	0.653±0.009	−5.86±0.30	−2.99±0.32
Model (Mixture B)[b]	N/A	0.657	−5.72	−3.09

All errors are 1 standard error.
[a]Number of replicate analyses.
[b]Errors and replicates are not computed for model outputs.

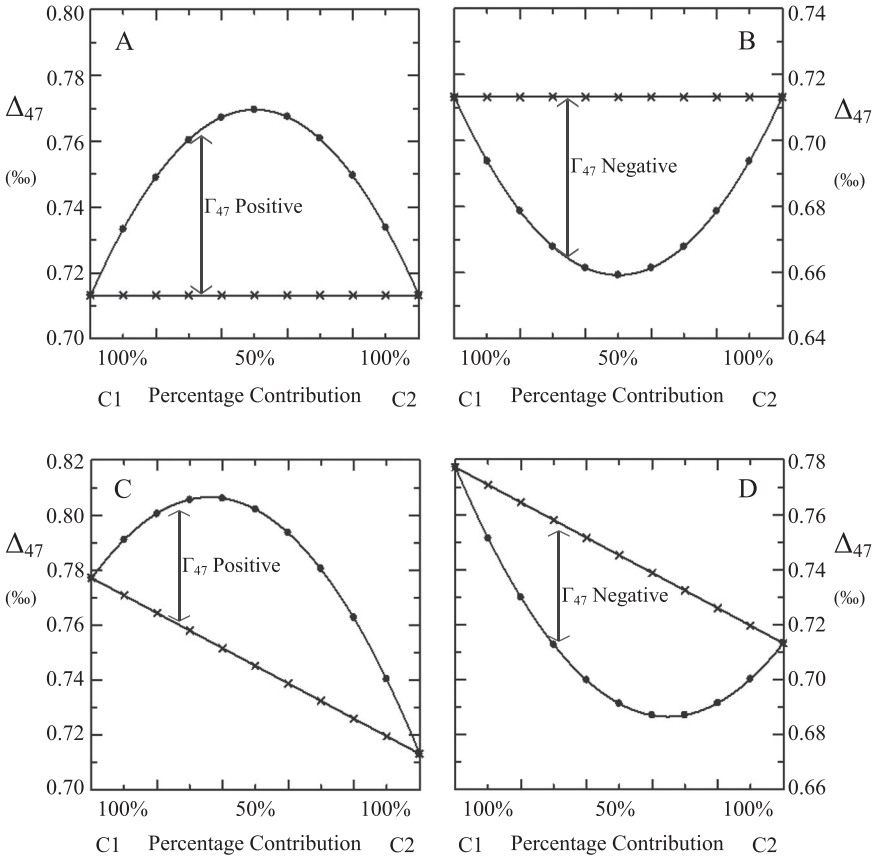

Figure 1. Changes in Γ_{47} as a function of percentage mixing. Δ_{47}-model results are given by circles, Δ_{47}-linear mixing by crosses. Component one (C1) and component two (C2) represent different end members, in each case component one and component two have different $\delta^{13}C$ and $\delta^{18}O$ values. (A) A positive Γ_{47} offset, caused by a positive correlation between $\delta^{13}C$ and $\delta^{18}O$ values, causes a temperature underestimate. C1 and C2 have the same Δ_{47} value. (B) A negative Γ_{47} offset, caused by a negative correlation between $\delta^{13}C$ and $\delta^{18}O$ values, results in a temperature overestimate. C1 and C2 have the same Δ_{47} value. (C) A positive Γ_{47} offset is manifest when C1 and C2 have differing Δ_{47} values. (D) A negative Γ_{47} offset occurring when C1 and C2 have differing Δ_{47} values.

however, as the model accurately predicted the final Δ_{47} value of each mixture. While these mixtures were specifically chosen from existing materials to create the largest possible positive and negative values of Γ_{47}, they illustrate the ability of end member mixing to significantly alter any interpretation that does not account for such offsets. For example, using the Δ_{47}–temperature scale of Ghosh *et al.*,[5] mixture B results in a 7.5 °C overestimate of temperature compared with the true temperature of formation (the average of the temperatures recorded by the end members). This demonstration shows that not only does mixing in Δ_{47} not follow linear trends, but that it can significantly affect temperature reconstructions and potentially lead to temperature over- or under-estimates, particularly when proxies of highly variable isotopic composition are used.

Implications for paleotemperature reconstructions

Our model results indicate that mixing can become a significant contribution to Δ_{47} when the sample exhibits isotopic heterogeneities of the order of ~2‰ or larger in carbon and oxygen ratios, or ~15‰ when only one isotope is involved. Since the sign of Γ_{47} cannot be determined without knowing the correlation between the $\delta^{13}C$ and $\delta^{18}O$ values, micro-sampling (possibly including the 'Kiel' technique for clumped isotope studies, as proposed by Schmid and Bernasconi,[20] or the dual reservoir technique of Petersen and Schrag[31]) is necessary to determine the magnitude and sign of any effect of mixing. A review of previous studies suggests that heterogeneities of the order of 2‰ or greater are likely to occur in several of the proxies commonly utilized for clumped isotope studies, including many biogenic carbonates (occurring as growth bands),[32–35] diagenetic carbonates,[15] and pedogenic carbonates.[36] Growth bands and diagenetic carbonates are well known to have isotopic variation, which can be especially large in the case of diagenetic carbonates.[37,38] Isotopic variation in pedogenic carbonates has been much less studied, with only a few examples of studies utilizing high-resolution measurements from individual soil nodules (eg, Duetz *et al.*[36]). Since pedogenic carbonates form over periods ranging from tens to millions of years, there is the potential for significant changes in precipitational environment recorded in

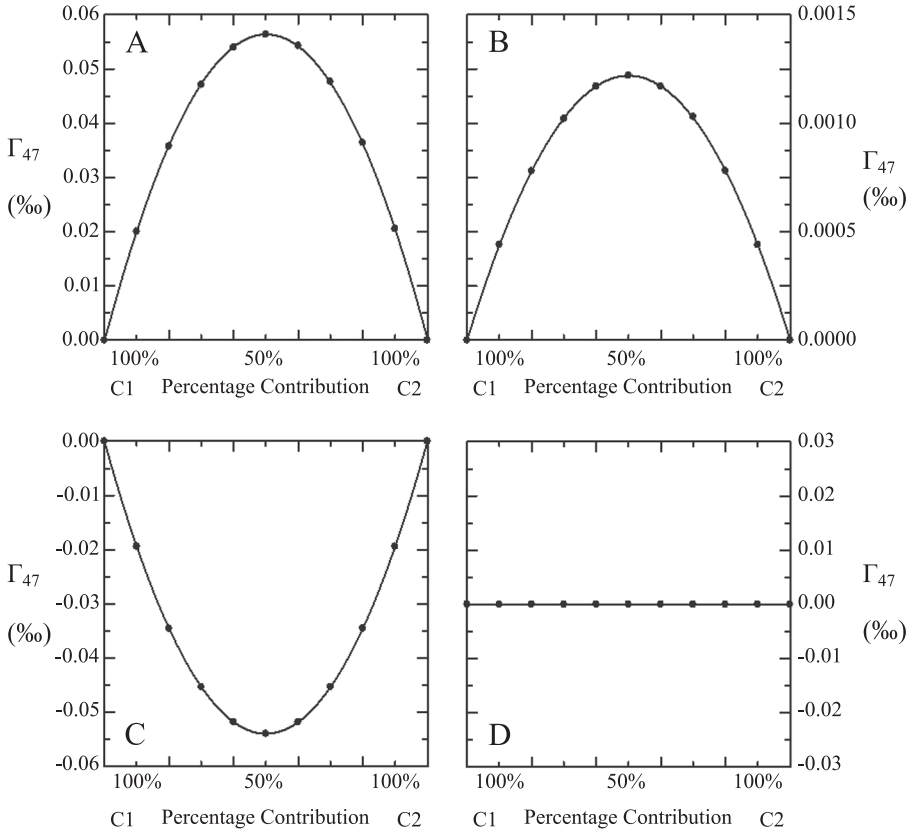

Figure 2. Demonstration of the different patterns of mixing, where component one (C1) and component two (C2) are carbonate end members with differing isotopic compositions. (A) A positive Γ_{47} occurs when there is a positive correlation between the $\delta^{13}C$ and $\delta^{18}O$ values of the end members. In this figure, Δ_{47} is constant, and the end members differ by 15‰ in both $\delta^{13}C$ and $\delta^{18}O$ values, with a positive correlation. (B) A positive Γ_{47} occurs when either the $\delta^{13}C$ or the $\delta^{18}O$ value is constant between the end members and the other varies; the effect is much smaller in magnitude than that shown in (A). (C) A negative Γ_{47} occurs when there is a negative correlation between the $\delta^{13}C$ and $\delta^{18}O$ values of the end members. In this figure, Δ_{47} is constant, and the end members differ by 15‰ in both carbon and oxygen values, with a negative correlation. (D) When the two end members have the same bulk isotopic composition, Γ_{47} is zero (no mixing offset).

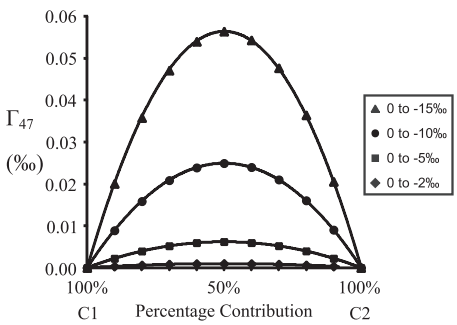

Figure 3. Illustration of the increasing size of Γ_{47} when the difference between end member compositions increases. In all cases, there is a positive correlation between the $\delta^{13}C$ and $\delta^{18}O$ values. In each case, component one has a composition of 0‰ for both $\delta^{13}C$ and $\delta^{18}O$, and component two has a composition for both $\delta^{13}C$ and $\delta^{18}O$ of −2‰ (diamonds), −5‰ (squares), −10‰ (circles), and −15‰ (triangles).

a single nodule.[39] Caliche profiles are often associated with internodule variation, with reported ranges as large as 3‰ in the $\delta^{18}O$ values and 11.3‰ in the $\delta^{13}C$ values between incipient nodules formed in the same unit.[40] This amount of variability is quite large, and thus caliche is not commonly utilized by paleopedogenic studies. Intranodule variation in non-caliche profiles have been studied by only a few authors, with the variability depending on the type of soil nodule. Zhou and Chafetz[40] found intranodule variability of up to 1.4‰ in the $\delta^{13}C$ values and 0.3‰ in the $\delta^{18}O$ values in non-altered soil nodules from a caliche profile, which is too small a variation to cause a mixing offset in clumped isotope measurements. In contrast, Bennett *et al.*[41] took transects across several soil nodules from Olduvai Gorge, Tanzania, and found that all had a positive correlation between the $\delta^{13}C$ and $\delta^{18}O$ values, with a maximum intranodule variability of up to 3.5‰ in the $\delta^{18}O$ values and 7.5‰ in the $\delta^{13}C$ values. Yang *et al.*[42] found a smaller variation in a single large nodule of 1.6‰ in the $\delta^{18}O$ values and 2.6‰ in the $\delta^{13}C$ values, but found a nearly 1:1 negative correlation between the $\delta^{18}O$ and $\delta^{13}C$ values. Variation exceeding 2‰ within individual nodules has also been reported by Duetz *et al.*[36] These contrasting results show that intranodule variability in soil carbonates can follow either positive or negative correlations, and may be large enough to cause statistically significant offsets in the

measured Δ_{47} values. Further study on the issue of intranodule variation would be beneficial to both the clumped isotope community and the broader paleopedology community, and may resolve some of the significant offsets observed between recorded temperatures and Δ_{47}-derived temperatures (e.g., Quade *et al.*[12]).

Application of the mixing model to clumped isotope results

To solve for Γ_{47}, it is necessary to know both the isotopic compositions of the end members and the percentage contribution of each end member to the mixture. As discussed previously, the Δ_{47} values of the end members do not contribute significantly to Γ_{47}, so it is not necessary to know them to calculate the true temperature of the mixture (i.e., the linear Δ_{47} value of the mixture). However, if one or more end member Δ_{47} values can be constrained, estimation of remaining end member Δ_{47} value can be calculated by mixing equations, enabling the system to be solved.

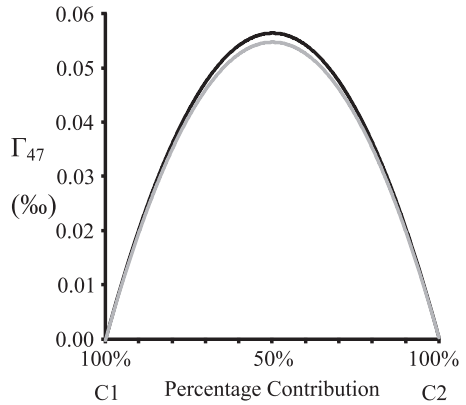

Figure 4. Illustration of the effect of differing absolute isotopic abundance on Γ_{47}. As there are fewer ^{13}C–^{18}O bonds overall, mixing creates a larger offset when they are less abundant (i.e., when both $\delta^{13}C$ and $\delta^{18}O$ values are very negative, giving less ^{13}C and ^{18}O in the whole system). The black line represents mixing between end members having compositions for both $\delta^{13}C$ and $\delta^{18}O$ of 0‰ for one end member and −15‰ for the other; the light grey line represents mixing between end members having compositions of 15‰ for one end member and 0‰ of the other in both $\delta^{13}C$ and $\delta^{18}O$.

Two-component systems

Two-component systems are easily solvable with a combination of Δ_{47} analysis, high-resolution $\delta^{18}O$ and $\delta^{13}C$ measurements, and/or knowledge of the percentage contributions to a mixture. Calculating the Γ_{47} of the mixture is straightforward, and can be accomplished in two ways: (1) knowledge of only the $\delta^{18}O$ and $\delta^{13}C$ values of both end members and the mixture, using Eqn. (17) to solve for the percentage contribution of each end member; or (2) knowledge of the isotopic values of one end member and of the mixture, and the percentage contribution of each end member to the mixture, then using Eqn. (17) to solve for the isotopic composition of the unknown end member. In practice, approach (1) is likely to be more accurate, but approach (2) can be used when the phases are too small to be sampled directly, with point counting or other techniques being used to estimate the percentage contribution to the mixture.

The Δ_{47} values for an end member can be extrapolated in a two-component system with knowledge of Γ_{47} for the mixture and constraints on the Δ_{47} value of the other end member. In this case, the linear Δ_{47} value of the mixture ($\Delta_{47linear}$) is obtained by subtracting Γ_{47} from the measured Δ_{47}. $\Delta_{47linear}$ can then be used in Eqn. (17) along with the known end member Δ_{47} value to estimate the Δ_{47} value of the other end member, since the percentage contribution of each end member is already known from the Γ_{47} calculation. There are numerous scenarios where this calculation might be useful, particularly in diagenetic environments where the formation temperature of one phase can be constrained by other methods (e.g., fluid inclusion thermometry), and the temperature of the other phase calculated using this approach.

Multiple-component systems

In the case of systems consisting of three or more components, solving for Γ_{47} requires knowledge of the end member isotopic compositions as well as an independent quantification of the percentage contributions to the mixture. It is possible through an algebraic approach to solve for the isotopic composition of a single unknown end member using Eqn. (17); however, the compositions of all other end members and the percentage contributions of each must be known. Solving for the Δ_{47} values for the end members is impossible except in the case of a single unknown end member, in which case Eqn. (17) may be applied.

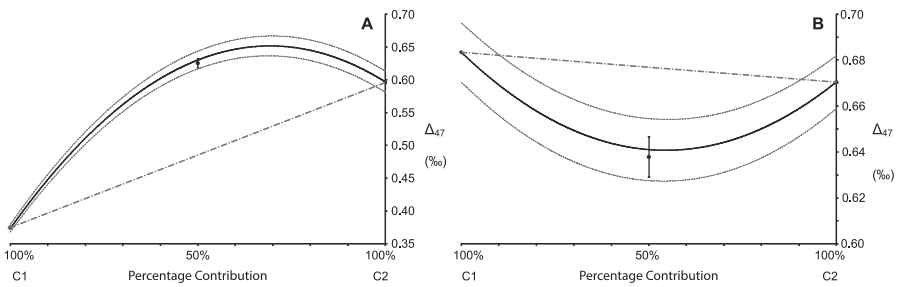

Figure 5. Modeled mixing results versus measured mixtures. Solid black line represents mean model results, with stippled grey lines showing the range of model output based on errors in end member values. Dashed grey line shows the pattern expected from linear mixing of Δ_{47}. Error bars are one standard error: (A) mixture A, representing a positive Γ_{47} and (B) mixture B, representing a negative Γ_{47}.

CONCLUSIONS

Model results on the effects of linear mixing of end members in mass-47 CO_2 clumped isotope analysis indicate that mixing offsets are usually not significant unless the variability in the $\delta^{18}O$ and $\delta^{13}C$ values exceeds 2‰ for both isotopes or 15‰ for a single isotope. The covariation between the $\delta^{18}O$ and $\delta^{13}C$ values control the sign of the Γ_{47} anomaly, as a positive correlation leads to an under-estimate of true precipitation temperatures, and a negative correlation leads to an over-estimate. End member Δ_{47} values have very little effect on the magnitude of Γ_{47}, suggesting that end member differences in $\delta^{18}O$ and $\delta^{13}C$ values are the primary influences on Γ_{47}. To quantify the effects of mixing on Δ_{47} measurements, it is suggested that high-resolution $\delta^{18}O$ and $\delta^{13}C$ analysis be performed on samples selected for clumped isotope thermometry when the samples are likely to show heterogeneity. Proxy materials that record seasonal environmental records or integrate large amounts of time in areas sampled for analysis are most likely to be affected by mixing.

Our results suggest that mixing alone is not responsible for many of the offsets between Δ_{47} values and estimated growth temperatures. However, proxies such as shells, corals, speleothems, soil carbonates, and diagenetic phases can all be subject to large variations in $\delta^{18}O$ and $\delta^{13}C$ values that can cause measureable Γ_{47} offsets. More research is needed to determine the natural variability within several of these materials. Further development of clumped isotope measurement techniques will probably lead to smaller sample sizes, lowering the risk of mixing multiple components into a single measurement.

Acknowledgements

WFD would like to thank Cedric John, who inspired this investigation via a conversation at the 2012 AGU Fall Meeting. The authors also thank Alex Lechler and Nathan Niemi for use of sample 10SP06A. This work was supported by NSF Geobiology and Low Temperature Geochemistry grant EAR 1123733 (KCL).

REFERENCES

[1] S. Zaarur, G. Olack, H. Affek. Paleo-environmental implication of clumped isotopes in land snail shells. *Geochim. Cosmochim. Acta* **2011**, *75*, 6859.
[2] G. A. Henkes, B. H. Passey, A. D. Wanamaker, E. L. Grossman, W. G. Ambrose, M. L. Carroll. Carbonate clumped isotope compositions of modern marine mollusk and brachiopod shells. *Geochim. Cosmochim. Acta* **2013**, *106*, 307.
[3] R. A. Eagle, J. M. Eiler, A. K. Tripati, J. B. Ries, P. S. Freitas, C. Hiebenthal, A. D. Wanamaker Jr., M. Taviani, M. Elliot, S. Marenssi, K. Nakamura, P. Ramirez, K. Roy. The influence of temperature and seawater carbonate saturation state on ^{13}C–^{18}O bond ordering in bivalve mollusks. *Biogeosciences* **2013**, *10*, 4591.
[4] R. E. Came, J. M. Eiler, J. Veizer, K. Azmy, U. Brand, C. R. Weidman. Coupling of surface temperatures and atmospheric CO_2 concentrations during the Palaeozoic era. *Nature* **2007**, *449*, 198.
[5] P. Ghosh, J. Adkins, H. Affek, B. Balta, W. F. Guo, E. A. Schauble, D. Schrag, J. M. Eiler. C-13-O-18 bonds in carbonate minerals: A new kind of paleothermometer. *Geochim. Cosmochim. Acta* **2006**, *70*, 1439.
[6] N. Thiagarajan, J. Adkins, J. Eiler. Carbonate clumped isotope thermometry of deep-sea corals and implications for vital effects. *Geochim. Cosmochim. Acta* **2011**, *75*, 4416.
[7] H. P. Affek, M. Bar-Matthews, A. Ayalon, A. Matthews, J. M. Eiler. Glacial/interglacial temperature variations in Soreq cave speleothems as recorded by 'clumped isotope' thermometry. *Geochim. Cosmochim. Acta* **2008**, *72*, 5351.
[8] T. Kluge, H. P. Affek. Quantifying kinetic fractionation in Bunker Cave speleothems using Δ47. *Quat. Sci. Rev.* **2012**, *49*, 82.
[9] A. K. Tripati, R. A. Eagle, N. Thiagarajan, A. C. Gagnon, H. Bauch, P. R. Halloran, J. M. Eiler. C-13-O-18 isotope signatures and 'clumped isotope' thermometry in foraminifera and coccoliths. *Geochim. Cosmochim. Acta* **2010**, *74*, 5697.
[10] J. Quade, C. Garzione, J. Eiler. Paleoelevation reconstruction using pedogenic carbonates, in *Paleoaltimetry: Geochemical and Thermodynamic Approaches. Reviews in Mineralogy & Geochemistry 66*. Mineralogical Society of America, Chantilly, VA, USA, **2007**, p. 53.
[11] B. H. Passey, N. E. Levin, T. E. Cerling, F. H. Brown, J. M. Eiler. High-temperature environments of human evolution in East Africa based on bond ordering in paleosol carbonates. *Proc. Natl. Acad. Sci.* **2010**, *107*, 11245.
[12] J. Quade, J. Eiler, M. Daëron, H. Achyuthan. The clumped isotope geothermometer in soil and paleosol carbonate. *Geochim. Cosmochim. Acta* **2013**, *105*, 92.
[13] R. A. Eagle, E. A. Schauble, A. K. Tripati, T. Tütken, R. C. Hulbert, J. M. Eiler. Body temperatures of modern and extinct vertebrates from 13C-18O bond abundances in bioapatite. *Proc. Natl. Acad. Sci.* **2010**, *107*, 10377.
[14] S. C. Bergman, K. W. Huntington, J. G. Crider. Tracing paleofluid sources using clumped isotope thermometry of diagenetic cements along the Moab Fault, Utah. *Am. J. Sci.* **2013**, *313*, 490.
[15] D. A. Budd, E. L. Frost, K. W. Huntington, P. F. Allwardt. Syndepositional deformation features in high-relief carbonate platforms: Long-lived conduits for diagenetic fluids. *J. Sediment. Res.* **2013**, *83*, 12.
[16] T. Bristow, M. Bonifacie, A. Derkowski, J. Eiler, J. Grotzinger. A hydrothermal origin for isotopically anomalous cap dolostone cements from south China. *Nature* **2011**, *474*, 68.
[17] J. Ferry, B. Passey, C. Vasconcelos, J. Eiler. Formation of dolomite at 40–80°C in the Latemar carbonate buildup, Dolomites, Italy, from clumped isotope thermometry. *Geology* **2011**, *39*, 571.
[18] K. W. Huntington, J. M. Eiler, H. P. Affek, W. Guo, M. Bonifacie, L. Y. Yeung, N. Thiagarajan, B. Passey, A. Tripati, M. Daëron, R. Came. Methods and limitations of 'clumped' CO2 isotope (Delta(47)) analysis by gas-source isotope ratio mass spectrometry. *J. Mass Spectrom.* **2009**, *44*, 1318.
[19] A. N. Meckler, M. Ziegler, M. I. Millán, S. F. M. Breitenbach, S. M. Bernasconi. Long-term performance of the Kiel carbonate device with a new correction scheme for clumped isotope measurements. *Rapid Commun. Mass Spectrom.* **2014**, *28*, 1705.
[20] T. W. Schmid, S. M. Bernasconi. An automated method for 'clumped-isotope' measurements on small carbonate samples. *Rapid Commun. Mass Spectrom.* **2010**, *24*, 1955.
[21] A. M. Zyakun. What factors can limit the precision of isotope ratio measurements in the isotopomer pool? *Int. J. Mass Spectrom.* **2003**, *229*, 217.
[22] J. M. Eiler, E. Schauble. (OCO)-O-18-C-13-O-16 in Earth's atmosphere. *Geochim. Cosmochim. Acta* **2004**, *68*, 4767.
[23] H. P. Affek, J. M. Eiler. Abundance of mass 47 CO_2 in urban air, car exhaust, and human breath. *Geochim. Cosmochim. Acta* **2006**, *70*, 1.
[24] J. Kaiser, T. Rockmann, C. A. M. Brenninkmeijer. Assessment of (NNO)-N-15-N-15-O-16 as a tracer of stratospheric processes. *Geophys. Res. Lett.* **2003**, *30*, 1046.
[25] K. J. Dennis, H. P. Affek, B. H. Passey, D. P. Schrag, J. M. Eiler. Defining an absolute reference frame for 'clumped' isotope studies of CO_2. *Geochim. Cosmochim. Acta* **2011**, *75*, 7117.

[26] P. K. Swart, S. J. Burns, J. J. Leder. Fractionation of the stable isotopes of oxygen and carbon in carbon dioxide during the reaction of calcite with phosphoric acid as a function of temperature and technique. *Chem. Geol.; Isot. Geosci. Sect.* **1991**, *86*, 89.
[27] R. Gonfiantini, W. Stichler, K. Rozanski. Standards and intercomparison materials distributed by the International Atomic Energy Agency for Stable Isotope Measurements, in *Reference and Intercomparison Materials for Stable Isotopes of Light Elements*. International Atomic Energy Agency, Vienna, Austria, **1993**.
[28] Z. G. Wang, E. A. Schauble, J. M. Eiler. Equilibrium thermodynamics of multiply substituted isotopologues of molecular gases. *Geochim. Cosmochim. Acta* **2004**, *68*, 4779.
[29] K. J. Dennis, D. P. Schrag. Clumped isotope thermometry of carbonatites as an indicator of diagenetic alteration. *Geochim. Cosmochim. Acta* **2010**, *74*, 4110.
[30] W. F. Defliese, M. T. Hren, K. C. Lohmann. Compositional and temperature effects of phosphoric acid fractionation on Δ_{47} analysis and implications for discrepant calibrations. *Chem. Geol.* **2015**, *396*, 51.
[31] S. V. Petersen, D. P. Schrag. Clumped isotope measurements of small carbonate samples using a high-efficiency dual-reservoir technique. *Rapid Commun. Mass Spectrom.* **2014**, *28*, 2371.
[32] J. F. Adkins, E. A. Boyle, W. B. Curry, A. Lutringer. Stable isotopes in deep-sea corals and a new mechanism for "vital effects". *Geochim. Cosmochim. Acta* **2003**, *67*, 1129.
[33] C. Rollion-Bard, J. Erez, T. Zilberman. Intra-shell oxygen isotope ratios in the benthic foraminifera genus Amphistegina and the influence of seawater carbonate chemistry and temperature on this ratio. *Geochim. Cosmochim. Acta* **2008**, *72*, 6006.
[34] H. U. I. Yan, X. Lee, H. U. I. Zhou, H. Cheng, Y. A. N. Peng, Z. Zhou. Stable isotope composition of the modern freshwater bivalve *Corbicula fluminea*. *Geochem. J.* **2009**, *43*, 379.
[35] M. T. Hren, N. D. Sheldon, S. T. Grimes, M. E. Collinson, J. J. Hooker, M. Bugler, K. C. Lohmann. Terrestrial cooling in Northern Europe during the Eocene–Oligocene transition. *Proc. Natl. Acad. Sci.* **2013**, *110*, 7562.
[36] P. Deutz, I. P. Montañez, H. C. Monger. Morphology and stable and radiogenic isotope composition of pedogenic carbonates in Late Quaternary relict soils, New Mexico, U.S.A.: An integrated record of pedogenic overprinting. *J. Sediment. Res.* **2002**, *72*, 809.
[37] N. P. James, P. W. Choquette. Limestones – the meteoric diagenetic environment, in *Diagenesis*, (Eds: I. A. McIlreath, D. W. Morrow). Geological Association of Canada, St. John's, Newfoundland, Canada, **1990**.
[38] P. W. Choquette, N. P. James. Limestones – the burial diagenetic environment, in *Diagenesis*, (Eds: I. A. McIlreath, D. W. Morrow). Geological Association of Canada, St. John's, Newfoundland, Canada, **1990**.
[39] N. D. Sheldon, N. J. Tabor. Quantitative paleoenvironmental and paleoclimatic reconstruction using paleosols. *Earth-Sci. Rev.* **2009**, *95*, 1.
[40] J. Zhou, H. S. Chafetz. Pedogenic carbonates in Texas: Stable-isotope distributions and their implications for reconstructing region-wide paleoenvironments. *J. Sediment. Res.* **2010**, *80*, 137.
[41] C. E. Bennett, J. D. Marshall, I. G. Stanistreet. Carbonate horizons, paleosols, and lake flooding cycles: Beds I and II of Olduvai Gorge. *Tanzania. J. Hum. Evol.* **2012**, *63*, 328.
[42] S. Yang, Z. Ding, X. Wang, Z. Tang, Z. Gu. Negative $\delta^{18}O$–$\delta^{13}C$ relationship of pedogenic carbonate from northern China indicates a strong response of C3/C4 biomass to the seasonality of Asian monsoon precipitation. *Palaeogeography, Palaeoclimatology, Palaeoecology* **2012**, *317/318*, 32.

SUPPORTING INFORMATION

Additional supporting information may be found in the online version of this article at the publisher's website.

APPENDIX A: Derivation of Eqn. (16)

We start with Eqn. (5) of Dennis *et al.*:[25]

$$\Delta_{47[\mathrm{SGvsWG}]0} = \Delta_{47[\mathrm{SGvsWG}]} - \delta^{47} \times \mathrm{EGL}_{\mathrm{Slope}} \tag{A1}$$

where $\Delta_{47[\mathrm{SGvsWG}]}$ is the raw uncorrected Δ_{47} value. We are attempting to rewrite this equation in order to solve for δ^{47}. To begin, we use Eqn. (19) to substitute for $\Delta_{47[\mathrm{SGvsWG}]}$:

$$\Delta_{47[\mathrm{SGvsWG}]0} = \left[\left(\frac{R^{47}}{R^{47^*}} - 1\right) - \left(\frac{R^{46}}{R^{46^*}} - 1\right) - \left(\frac{R^{45}}{R^{45^*}} - 1\right)\right] \times 1000 - \delta^{47} \times \mathrm{EGL}_{\mathrm{Slope}} \tag{A2}$$

To proceed with the calculation, it is assumed that only δ^{47} contributes to Δ_{47}. This is necessary to solve the equation as otherwise there are too many unknowns, and such an assumption contributes little error into the calculation, as described in the text. In this case, R^{46}/R^{46^*} and R^{45}/R^{45^*} are assumed to each equal 1. Therefore:

$$\Delta_{47[\mathrm{SGvsWG}]0} = \left[\frac{R^{47}}{R^{47^*}} - 1\right] \times 1000 - \delta^{47} \times \mathrm{EGL}_{\mathrm{Slope}} \tag{A3}$$

Equation (18) is then substituted for R^{47} in order to describe it in terms of δ^{47}:

$$\Delta_{47[\mathrm{SGvsWG}]0} = \left[\frac{\left(\frac{\delta 47}{1000} + 1\right) \times R^{47^*}_{\mathrm{WG}}}{R^{47^*}} - 1\right] \times 1000 - \delta^{47} \times \mathrm{EGL}_{\mathrm{Slope}} \tag{A4}$$

From here it is a matter of rearranging the terms to solve for δ^{47} in terms of the other variables, all of which are known:

$$\Delta_{47[\mathrm{SGvsWG}]0} = \delta^{47} \times \left(\frac{R^{47^*}_{\mathrm{WG}}}{R^{47^*}} - \mathrm{EGL}_{\mathrm{Slope}}\right) + 1000 \times \frac{R^{47^*}_{\mathrm{WG}}}{R^{47^*}} - 1000 \tag{A5}$$

$$\Delta_{47[\mathrm{SGvsWG}]0} + 1000 - 1000 \times \frac{R^{47^*}_{\mathrm{WG}}}{R^{47^*}} = \delta^{47} \times \left(\frac{R^{47^*}_{\mathrm{WG}}}{R^{47^*}} - \mathrm{EGL}_{\mathrm{Slope}}\right) \tag{A6}$$

Both sides are multiplied by R^{47^*} for convenience:

$$\left(\Delta_{47[\mathrm{SGvsWG}]0} + 1000\right) \times R^{47^*} - 1000 \times R^{47^*}_{\mathrm{WG}} = \delta^{47} \times \left(R^{47^*}_{\mathrm{WG}} - \mathrm{EGL}_{\mathrm{Slope}} \times R^{47^*}\right) \tag{A7}$$

A final rearrangement yields Eqn. (16):

$$\delta^{47} = \frac{\left(\Delta_{47[\mathrm{SGvsWG}]0} + 1000\right) \times R^{47^*} - 1000 \times R^{47^*}_{\mathrm{WG}}}{R^{47^*}_{\mathrm{WG}} - \mathrm{EGL}_{\mathrm{Slope}} \times R^{47^*}} \tag{A8}$$

